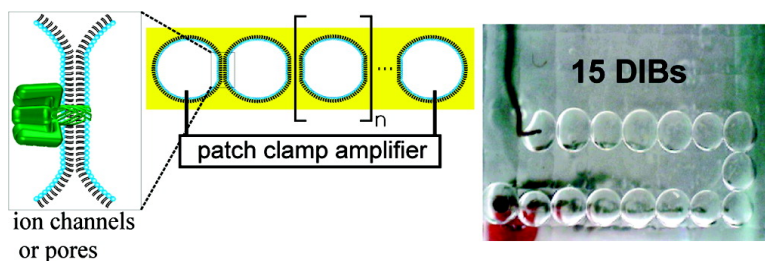


## Functional Bionetworks from Nanoliter Water Droplets

Matthew A. Holden, David Needham, and Hagan Bayley

*J. Am. Chem. Soc.*, **2007**, 129 (27), 8650-8655 • DOI: 10.1021/ja072292a • Publication Date (Web): 16 June 2007

Downloaded from <http://pubs.acs.org> on February 16, 2009



### More About This Article

Additional resources and features associated with this article are available within the HTML version:

- Supporting Information
- Links to the 11 articles that cite this article, as of the time of this article download
- Access to high resolution figures
- Links to articles and content related to this article
- Copyright permission to reproduce figures and/or text from this article

[View the Full Text HTML](#)



## Functional Bionetworks from Nanoliter Water Droplets

Matthew A. Holden,<sup>\*,†</sup> David Needham,<sup>‡</sup> and Hagan Bayley<sup>†</sup>

Contribution from the Department of Chemistry, University of Oxford, Chemistry Research Laboratory, Mansfield Road, OX1 3TA Oxford, U.K., and Department of Mechanical Engineering and Materials Science, Duke University, Durham, North Carolina

Received April 10, 2007; E-mail: matthew.holden@chem.ox.ac.uk

**Abstract:** We form networks from aqueous droplets by submerging them in an oil/lipid mixture. When the droplets are joined together, the lipid monolayers surrounding them combine at the interface to form a robust lipid bilayer. Various protein channels and pores can incorporate into the droplet-interface bilayer (DIB), and the application of a potential with electrodes embedded within the droplets allows ionic currents to be driven across the interface and measured. By joining droplets in linear or branched geometries, functional bionetworks can be created. Although the interfaces between neighboring droplets comprise only single lipid bilayers, the structures of the networks are long-lived and robust. Indeed, a single droplet can be "surgically" excised from a network and replaced with a new droplet without rupturing adjacent DIBs. Networks of droplets can be powered with internal "biobatteries" that use ion gradients or the light-driven proton pump bacteriorhodopsin. Besides their interest as coupled protocells, the droplets can be used as devices for ultrastable bilayer recording with greatly reduced electrolyte volume, which will permit their use in rapid screening applications.

## Introduction

The practice of joining two lipid monolayers to create a suspended bilayer began with Montal and Mueller more than 30 years ago.<sup>1</sup> In an approach still widely used today, planar bilayers are formed by raising two Langmuir–Blodgett monolayers across a plastic aperture. Recently, a new technique for contacting two monolayers has emerged.

Funakoshi et al. describe both a droplet-based and a microfluidic approach for creating bilayers between two aqueous volumes immersed in or separated by an oil/lipid mixture.<sup>2</sup> A similar microfluidic approach was described by Malmstadt et al.<sup>3</sup> We have worked in parallel on the droplet-based approach and describe our findings here.

Although an extensive body of literature can be found describing reverse micelles and water-in-oil emulsions, the recent work of Funakoshi et al. is the first to describe the formation of bilayers from monolayer-encased droplets in oil, as well as the study of individual ion-conducting membrane proteins embedded in these bilayers. The robustness of either the droplet-based or microfluidic bilayer methods was not documented; neither group reported the average lifetimes of the bilayers during electrical recording, and the longest traces shown in these papers were only seconds long. Although the microfluidic approach was suitable for creating single bilayer inter-

faces, recordings through multiple interfaces in these systems were not achieved. In contrast to the work presented here, the enclosed microchannels hinder accessibility to the droplets and prevent the manipulation and reorganization of droplet networks.

Recently, substantial progress has been made in the creation of artificial "protocells" that incorporate biological functions, such as gene transcription,<sup>4–6</sup> protein synthesis,<sup>7</sup> cell division,<sup>8–10</sup> selective uptake of small molecules,<sup>11,12</sup> and energy production and storage.<sup>13–15</sup> Although observations made using these systems have provided biological and evolutionary insight,<sup>16–18</sup> the assembly of protocells into communicating and functional networks has not yet been realized. It would be highly desirable to create robust, microscale systems with multiple bilayer interfaces that can be extended or rearranged at will.

- (4) Fischer, A.; Franco, A.; Oberholzer, T. *ChemBioChem* **2002**, *3*, 409–417.
- (5) Noireaux, V.; Bar-Ziv, R.; Godefroy, J.; Salman, H.; Libchaber, A. *Phys. Biol.* **2005**, *2*, P1–P8.
- (6) Luisi, P. L.; Ferri, F.; Stano, P. *Naturwissenschaften* **2006**, *93*, 1–13.
- (7) Pietrini, A. V.; Luisi, P. L. *ChemBioChem* **2004**, *5*, 1055–1062.
- (8) Luisi, P. L.; Stano, P.; Rasi, S.; Mavelli, F. *Artif. Life* **2004**, *10*, 297–308.
- (9) Hanczyc, M. M.; Szostak, J. W. *Curr. Opin. Chem. Biol.* **2004**, *8*, 660–664.
- (10) Chen, I. A.; Salehi-Ashtiani, K.; Szostak, J. W. *J. Am. Chem. Soc.* **2005**, *127*, 13213–13219.
- (11) Noireaux, V.; Libchaber, A. *Proc. Natl. Acad. Sci. U.S.A.* **2004**, *101*, 17669–17674.
- (12) Deamer, D. *Trends Biotechnol.* **2005**, *23*, 336–338.
- (13) Bennett, I. M.; Farfano, H. M. V.; Bogani, F.; Primak, A.; Liddell, P. A.; Otero, L.; Sereno, L.; Silber, J. J.; Moore, A. L.; Moore, T. A.; Gust, D. *Nature* **2002**, *420*, 398–401.
- (14) Luo, T. J. M.; Soong, R.; Lan, E.; Dunn, B.; Montemagno, C. *Nat. Mater.* **2005**, *4*, 220–224.
- (15) Bhosale, S.; Sisson, A. L.; Talukdar, P.; Furstenberg, A.; Banerji, N.; Vauthey, E.; Bollot, G.; Mareda, J.; Roger, C.; Wurthner, F.; Sakai, N.; Matile, S. *Science* **2006**, *313*, 84–86.
- (16) Tawfik, D. S.; Griffiths, A. D. *Nat. Biotechnol.* **1998**, *16*, 652–656.
- (17) Szostak, J. W.; Bartel, D. P.; Luisi, P. L. *Nature* **2001**, *409*, 387–390.
- (18) Rasmussen, S.; Chen, L. H.; Deamer, D.; Krakauer, D. C.; Packard, N. H.; Stadler, P. F.; Bedau, M. A. *Science* **2004**, *303*, 963–965.

<sup>†</sup> University of Oxford.<sup>‡</sup> Duke University.

- (1) Montal, M.; Mueller, P. *Proc. Natl. Acad. Sci. U.S.A.* **1972**, *69*, 3561–3566.
- (2) Funakoshi, K.; Suzuki, H.; Takeuchi, S. *Anal. Chem.* **2006**, *78*, 8169–8174.
- (3) Malmstadt, N.; Nash, M. A.; Purnell, R. F.; Schmidt, J. J. *Nano Lett.* **2006**, *6*, 1961–1965.

Herein, we describe the creation of droplet–interface bilayer (DIB) networks as model systems for the study of membrane-based biological phenomena. Each droplet is a self-contained unit of a larger overall system. The interfaces between droplets are robust bilayers which enable electrical recording through incorporated membrane channels and pores for several days. The DIB networks are studied by measuring ionic currents using electrodes, which are inserted into the droplets. By rearranging the droplets in a network, the overall functional properties of the network can be changed. We used the DIB system to build functional linear and branched networks that act as wires, batteries, or light sensors. In addition, we demonstrate the utility of DIBs for high-throughput membrane protein screening.

## Results and Discussion

We used a solution of 10 mM 1,2-diphytanoyl-*sn*-glycero-3-phosphocholine (DPhPC) in hexadecane as the bathing medium in all experiments. Funakoshi et al. used the same lipid but dissolved it in *n*-decane instead of hexadecane.<sup>2</sup> Initially, we found that when two 200 nL water droplets were placed under the oil/lipid solution and brought immediately into contact, they fused into a single droplet in less than 1 min. We hypothesized that more time was needed to allow a densely packed well-ordered monolayer to form.<sup>19</sup> Therefore, two strategies were developed to augment this process, which we term stabilization (for more detail, see the Supporting Information). In the first approach, two or more droplets were kept separated under the oil/lipid bath for 30 min before joining them together. The second approach used a straight 20 cm section of 1.59 mm i.d. tubing that was filled with the oil/lipid mixture and closed at one end. With the open end up, droplets were pipetted into the top, just under the oil surface, and allowed to fall nearly to the bottom of the tube. The tube was then inverted, causing the droplet to descend toward the open end. Just before the droplet reached the opening, the tube was brought into contact with the surface of an oil/lipid bath so that the droplet landed on the bottom of the bath.

Using the latter technique, we created a network of 20 droplets on a Perspex surface with a square array of micromachined dimples (a miniature “egg-crate”, Figure 1). Each droplet contained either tetramethylrhodamine (pink) or Alexa 488 linked to a dextran polymer (yellow), in 10 mM MOPS, 1 M KCl, pH 7.0. When a droplet was added, it “clicked” together with its neighbor(s) as the interstitial oil was displaced. The interface between the droplets was stable to mechanical perturbation. Indeed, we were able to puncture into a droplet and then extract it from the network by using an agarose gel-coated Ag/AgCl electrode controlled by micromanipulator (pink droplet, Figure 1, parts b and c, and Supporting Information Video 1). Further, we could replace the missing droplet by stabilizing and dropping a yellow droplet into the empty position. This droplet spontaneously integrated into the network (Figure 1d, also see Supporting Information Video 2). Remarkably then, components of droplet networks can be extracted and exchanged without compromising the integrity of the surrounding system.

If the structure of the droplet interface is indeed a lipid bilayer, then pores or ion channels should insert and function in it. To test this hypothesis, we created a single bilayer using two

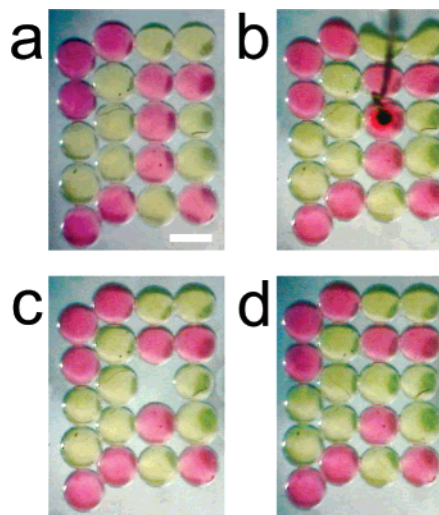


**Figure 1.** The droplet–interface bilayer (DIB) network. Twenty droplets were arranged on a Perspex surface with a square array of indentations under 10 mM DPhPC in hexadecane. Bright-field images were taken from above through one eyepiece of a stereomicroscope using a digital camera. Tetramethylrhodamine (0.6  $\mu$ M) and Alexa488 linked to dextran (0.2  $\mu$ M) were used to provide color. Both were dissolved in 10 mM MOPS, 1 M KCl, pH 7.0. (a) Droplets were stabilized (see the text) separately and then transferred one-at-a-time to form a pattern. Lipid bilayers formed at each of the droplet–droplet interfaces. The scale bar is 700  $\mu$ m. (b) An agarose-coated Ag/AgCl electrode ( $\sim$ 200  $\mu$ m in diameter) attached to a micromanipulator was used to puncture and withdraw a droplet from the network. (c) The network was not damaged by removal of the droplet. (d) A yellow droplet was stabilized and then added to the network to replace the droplet that had been removed (see also Supporting Information Videos 1 and 2).

200 nL droplets (Figure 2a). These were kept separated on Ag/AgCl electrodes to allow monolayer formation (Figure 2b). After 30 min, the droplets were brought into contact and a bilayer formed as monitored by capacitance measurements (Figure 2c). The area of the bilayer was controlled by using the micromanipulator. Pushing the droplets together resulted in a larger area, while pulling the droplets reduced the bilayer area. Using a specific capacitance of 0.65  $\mu$ F/cm<sup>2</sup>, we estimated the contact area between droplets (the measured capacitance value was  $\sim$ 300 pF) to be  $\sim$ 450  $\mu$ m<sup>2</sup>. The left-hand droplet contained 10 pg/mL wild-type (WT) staphylococcal  $\alpha$ -hemolysin ( $\alpha$ HL) heptamer in 10 mM MOPS, 1 M KCl, pH 7.0, whereas the right-hand droplet contained 10  $\mu$ M  $\gamma$ -cyclodextrin ( $\gamma$ CD) also in 10 mM MOPS, 1 M KCl, pH 7.0. The  $\gamma$ CD binds to the heptameric pore and acts as a reversible blocker,<sup>20–22</sup> which serves as a diagnostic tool to show that increases in current during an applied potential are due to pore insertion rather than current leakage through the droplet/droplet interface. Pore insertion into the bilayer was observed as a characteristic increase in ionic current at  $-50$  mV. The conductance of a single  $\alpha$ HL pore in a DIB was  $798 \pm 70$  pS ( $n = 6$ ), similar to a previously reported value of 775 pS (5 mM HEPES, 1 M KCl, pH 7.4) obtained using a folded planar bilayer.<sup>23</sup> In the presence of  $\gamma$ CD, transient blockades of the current were observed (Figure 2d), which were attributed to  $\gamma$ CD binding events. The residence time ( $\tau_{\text{off}}$ ) for  $\gamma$ CD bound to the  $\alpha$ HL pore was  $495 \pm 51$  ms

(20) Gu, L. Q.; Braha, O.; Conlan, S.; Cheley, S.; Bayley, H. *Nature* **1999**, *398*, 686–690.

(21) Gu, L. Q.; Cheley, S.; Bayley, H. *J. Gen. Physiol.* **2001**, *118*, 481–493.

(22) Gu, L. Q.; Cheley, S.; Bayley, H. *Science* **2001**, *291*, 636–640.

(23) Miles, G.; Cheley, S.; Braha, O.; Bayley, H. *Biochemistry* **2001**, *40*, 8514–8522.

(19) Needham, D.; et al. Manuscript in preparation.

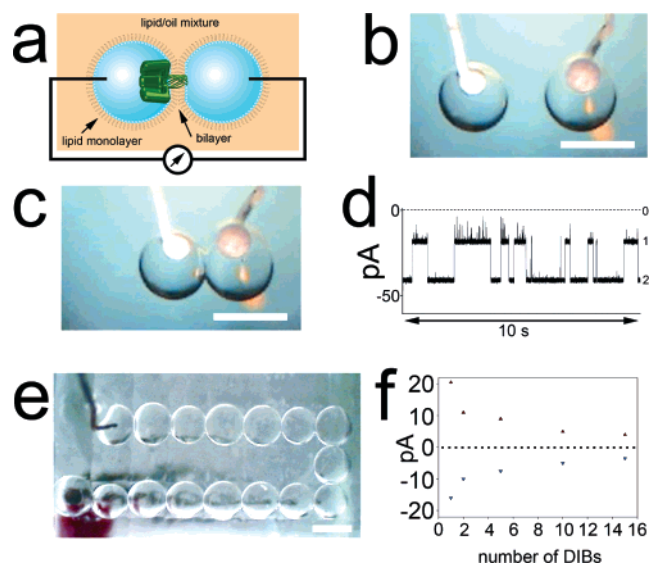


**Figure 2.** Recording through proteins in single or multiple DIBs. (a) Single bilayers were formed by hanging a pair of droplets from electrodes, one of which was movable, under an oil/lipid mixture. (b) Bright-field image showing two droplets ( $\sim 200$  nL each) suspended from electrodes; the scale bar is  $700 \mu\text{m}$ . (c) The droplets were kept apart for 30 min (no current was observed while the droplets were separated) and then brought into contact using a micromanipulator. Bilayer formation was observed as an increase in capacitance. Pores or channels inside one of the droplets inserted into the DIB and electrical measurements were made. (d) Ionic current recording showing  $50 \mu\text{M}$   $\gamma\text{CD}$  reversibly binding to a WT  $\alpha\text{HL}$  pore. Current levels 0, 1, and 2 represent, respectively, the current at 0 mV, the current through the pore with  $\gamma\text{CD}$  bound, and the current through the open pore at  $-50$  mV in 10 mM MOPS, 1 M KCl, pH 7.0. (e) Measuring ionic current across multiple bilayers. Each 200 nL droplet contained 10 mM HEPES, 100 mM NaCl, pH 7.5 with 17 ng/mL WT  $\alpha\text{HL}$  heptamer. Droplets were stabilized separately and deposited one-at-a-time on a Perspex surface with a square array of micromachined dimples (scale bar,  $700 \mu\text{m}$ ). The first droplet (number 0, bottom left) was situated on a stationary Ag/AgCl electrode and the last (droplet 15, top left) was pierced by a movable electrode. (f) Steady-state currents at  $\pm 50$  mV as a function of the number of bilayers between the electrodes. The dashed line represents current at 0 mV.

( $n = 4$ ), similar to the residence time ( $\tau_{\text{off}} = 421 \pm 22$  ms,  $n = 4$ ) found in control experiments using the same protein in a folded bilayer under the same solution conditions. In this way, we have demonstrated that the interface between the droplets is indeed a lipid bilayer.

The creation of additional DIBs is easily accomplished by connecting stabilized droplets to create a chain. We arranged 16 droplets (15 DIBs) in a row on the dimpled Perspex surface (Figure 2e). The first droplet in the chain was arranged on a fixed electrode. With the use of a micromanipulator, the opposing Ag/AgCl electrode ( $100 \mu\text{m}$  in diameter) could be plugged into any droplet in the chain. Each 200 nL droplet contained 10 mM HEPES, 100 mM NaCl, pH 7.5, and 17 ng/mL WT  $\alpha\text{HL}$  heptamer. The movable electrode was first plugged into the last droplet, and a current recording at  $\pm 50$  mV was performed. The electrode was then retracted, moved up the chain by five droplets, and plugged in. We found that the current decreased sharply as a function of the number of interfaces across which the potential was applied (Figure 2f). This demonstrates that electrodes can be inserted and withdrawn from the network at any location, thereby allowing complex networks to be studied either as a whole or in smaller sections.

The ability to interconnect stable, nanoliter compartments using protein gateways forms the basis for the creation of a

rudimentary artificial multicellular system.<sup>9–11,24</sup> Living cells carry out the functions of life in separate compartments, which communicate in part through channels and pores. Networks of droplets interfaced through DIBs might be designed to mimic these processes. The  $\alpha\text{HL}$  protein pore is an excellent starting point, because it adopts a known orientation in a bilayer. Further, the properties of the pore, such as unitary conductance, ion selectivity, rectification, gating, interactions with blockers, and selective transport of small molecules, can be tailored through genetic engineering to provide specific functions in a network.<sup>20,22,25,26</sup> For example, an ionic gradient might be combined with an ion-selective pore to generate a transmembrane potential across one droplet interface, which in turn could be used to power processes occurring at a droplet interface farther along a DIB chain.

We demonstrated the latter concept by using a three droplet chain (Figure 3a). Droplet D contained the N123R  $\alpha\text{HL}$  homoheptamer (in 10 mM HEPES, 100 mM NaCl, pH 7.5), which is moderately anion selective.<sup>27</sup> Droplet E contained 10 mM HEPES, 1 M NaCl, pH 7.5, and droplet F contained  $10 \mu\text{M}$   $\beta\text{CD}$  and the M113F/K147N  $\alpha\text{HL}$  homoheptamer<sup>28</sup> in 10 mM HEPES, 1 M NaCl, pH 7.5. Droplets D and F were hung from stationary Ag/AgCl electrodes that were connected to a patch-clamp amplifier, while droplet E was hung from a movable wire. After stabilization, droplet E was moved into position between droplets D and F to induce the formation of both bilayers. After pore insertion at both interfaces, the N123R pores allowed a higher flux of  $\text{Cl}^-$  relative to  $\text{Na}^+$  ions from E to D, which provided approximately  $+30$  mV at the EF interface as estimated by using the Goldman–Hodgkin–Katz equation. The power supplied by the “biobattery” formed by the D and E droplets enabled the observation of blocking events at the EF interface, where M113F/K147N pores reversibly bound  $\beta\text{CD}$  (Figure 3b). We emphasize that the patch clamp amplifier was not used to apply a potential, rather it was only used to record current.

The properties of a network can be modified by changing its geometry. For example, we constructed a branched “biobattery” from six 200 nL droplets using the same ionic gradient as above (Figure 3c, left). Three droplets (red) contained N123R  $\alpha\text{HL}$  homoheptamer (in 10 mM HEPES, 100 mM NaCl, pH 7.5, 1.8 M sucrose) and were situated on the termini of a common branched electrode. These interfaced with three sides of a droplet (blue) containing only 10 mM HEPES, 1 M NaCl, pH 7.5. The remaining side of the blue droplet was linked to a short chain of droplets (green) containing 17 ng/mL WT  $\alpha\text{HL}$  heptamer in 10 mM HEPES, 1 M NaCl, pH 7.5. The opposing electrode was plugged into the terminal  $\alpha\text{HL}$  droplet. When all the red droplets were connected with the blue droplet, a high current ( $\sim -390$  pA) was recorded (Figure 3c, right). As indicated by the first arrow, droplet 1 was then removed from the network, which caused the current to drop to  $\sim -61$  pA. Removal of droplet 2 caused a further decrease in current to  $\sim -21$  pA. Finally, when the third droplet was removed no current was observed. In this example, the function of the network was

(24) Chen, I. A.; Roberts, R. W.; Szostak, J. W. *Science* **2004**, *305*, 1474–1476.

(25) Bayley, H.; Cremer, P. S. *Nature* **2001**, *413*, 226–230.

(26) Bayley, H.; Jayasinghe, L. *Mol. Membr. Biol.* **2004**, *21*, 209–220.

(27) Madathil, R.; et al. Manuscript in preparation.

(28) Kang, X. F.; Gu, L. Q.; Cheley, S.; Bayley, H. *Angew. Chem., Int. Edit.* **2005**, *44*, 1495–1499.

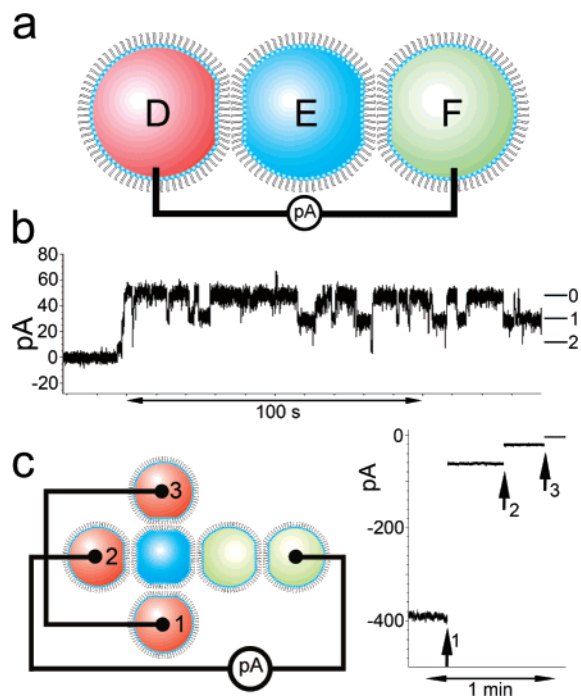


**Figure 3.** The “biobattery.” (a) Three droplets were arranged as follows: Droplet D (10 mM HEPES, 100 mM NaCl, pH 7.5) contained the anion-selective N123R  $\alpha$ HL pore. Droplet E contained 10 mM HEPES, 1 M NaCl, pH 7.5, and droplet F contained 10  $\mu$ M  $\beta$ CD and M113F/K147N  $\alpha$ HL in 10 mM HEPES, 1 M NaCl, pH 7.5. Droplets D and F were placed on opposing electrodes, which were electrically balanced before the start of the experiment. (b) Following the insertion of two pores at the EF interface, the power supplied by the “biobattery” enabled the observation of reversible  $\beta$ CD current blocks. Current levels 0, 1, and 2 indicate both pores open, one pore open and one pore partially blocked, and both pores partially blocked by  $\beta$ CD, respectively. (c) Droplets 1, 2, and 3 (red) were each situated on a terminus of a common branched electrode and contained 10 mM HEPES, 100 mM NaCl, pH 7.5, 1.8 M sucrose, and N123R  $\alpha$ HL. These were attached to a central droplet containing 10 mM HEPES, 1 M NaCl, pH 7.5 (blue). Finally, two droplets (green) containing 17 ng/mL WT  $\alpha$ HL heptamer in 10 mM HEPES, 1 M NaCl, pH 7.5 were arranged in series with the blue droplet, with the opposing electrode in the terminal green droplet. The trace on the right shows the current generated by the battery. At arrow 1, the Faraday box was opened and droplet 1 was pulled from the network, and the subsequent decrease in current was recorded. The electrical noise caused during this process (which took about 20 s, see text) was deleted from the trace for clarity. When droplet 2 was removed (scan, arrow 2), the current further decreased. When droplet 3 was removed, the current was abolished. Because the pores were randomly distributed in the DIBs, the magnitude of the current drop with each droplet removed varied from experiment to experiment.

changed by removing droplets. However, connecting, rearranging, or exchanging droplets can also be used to alter network properties.

Nature’s ability to receive and transmit information gathered from stimuli is enabled by differentiated cells working collectively. The retina, for example, senses light using rod and cone cells, which initiate a cascade of processes that transmit information down the optic nerve for interpretation by the brain. In a rudimentary mimic of this biosystem, we constructed a light-sensing network based on the light-driven proton pump, bacteriorhodopsin (BR).<sup>29</sup> Three droplets were placed on the termini of a common electrode and contained 10 mM HEPES, 100 mM NaCl, pH 7.5, 0.001% dodecylmaltoside (DDM) and 18  $\mu$ M BR (Figure 4a, purple droplets). A central droplet contained 10 mM HEPES, 100 mM NaCl, pH 7.5 (blue), while

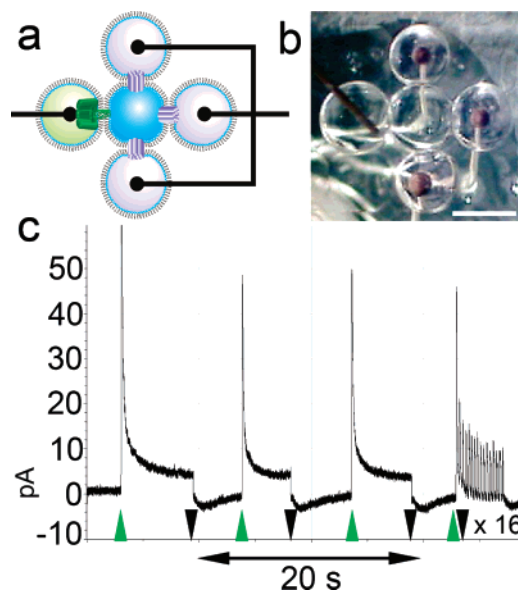


**Figure 4.** Light-sensing DIB network. (a) Three droplets (purple) containing 18  $\mu$ M bacteriorhodopsin (BR) in 10 mM HEPES, 100 mM NaCl, pH 7.5, and 0.001% DDM were deposited onto three branches of a common electrode. The central droplet (blue) contained 10 mM HEPES, 100 mM NaCl, pH 7.5. The droplet fixed to the opposite electrode (green) contained 10 mM HEPES, 100 mM NaCl, pH 7.5, with 17 ng/mL WT  $\alpha$ HL heptamer. (b) Bright-field image of (a); the scale bar is 700  $\mu$ m. A green pen laser (532 nm, 1 mW) illuminated an area slightly larger than the five-droplet network. (c) Electrical recording during laser illumination; ( $\blacktriangle$ ) indicates laser on for  $\sim$ 5 s followed by ( $\blacktriangledown$ ) laser off for  $\sim$ 5 s. At the end of the trace, the laser pen’s button was rapidly depressed and released to create a short train of light pulses, which are reflected in the electrical recording.

the final outer droplet contained 10 mM HEPES, 100 mM NaCl, pH 7.5 with 17 ng/mL WT  $\alpha$ HL heptamer (green). The opposing electrode was plugged into the  $\alpha$ HL droplet. A bright-field image of this array is shown in Figure 4b. A 1 mW green (532 nm) pen laser was used to illuminate the network. Three cycles of 5 s on/5 s off were performed, followed by a rapid sequence of 16 laser pulses. When the laser was switched on, a sharp spike in current was observed, which quickly decayed to  $\sim$ 5 pA after 5 s (Figure 4c). Switching the laser off caused the current to dip briefly to a negative value before returning to zero. Similar observations of BR behavior have been observed using a planar bilayer.<sup>30,31</sup> Each BR transports one proton across the membrane per photon of light absorbed, thus generating a current.<sup>29</sup> A 5 pA current suggests that tens of thousands of molecules must be functioning in the DIB membranes. As a control, the BR droplets were replaced with droplets containing only buffer, and the experiment was repeated. We found that although the electrode surfaces were exposed to the laser during illumination, no current from a photoelectric effect was observed in our system. In this example, each BR droplet “senses” light by generating a current. The collective function of the three BR droplets sum to create a “signal” that is interpreted by a patch-clamp amplifier and computer. Larger networks might be constructed with clusters of BR droplets which could then act as pixels in an imaging array.

The need to rapidly screen for diseases caused by defective ion channels presents a daunting challenge in the area of channelopathies.<sup>32</sup> Although ion channels, such as Na<sup>+</sup>, K<sup>+</sup>,

(30) Dancshazy, Z.; Karvaly, B. *FEBS Lett.* **1976**, *72*, 136–138.

(31) Horn, C.; Steinem, C. *Biophys. J.* **2005**, *89*, 1046–1054.

(32) Ashcroft, F. M. *Nature* **2006**, *440*, 440–447.

(29) Lanyi, J. K. *Biochim. Biophys. Acta: Bioenerg.* **2006**, *1757*, 1012–1018.

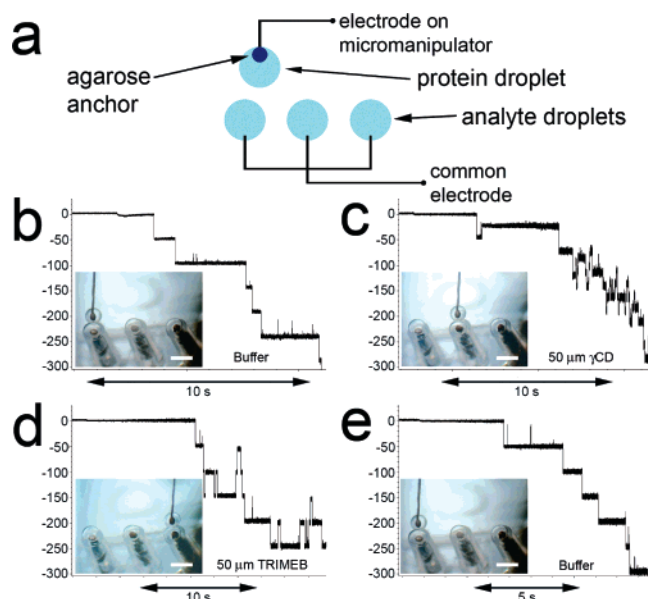


**Figure 5.** Screening pore blockers using a droplet array. (a) An  $\alpha$ HL droplet was placed on the movable electrode while the opposing branched electrode was common to the three analyte droplets. The first droplet contained only 10 mM MOPS, 1 M KCl, pH 7.0, the second contained 50  $\mu$ M  $\gamma$ CD in 10 mM MOPS, 1 M KCl, pH 7.0, and the third contained 50  $\mu$ M TRIMEB in 10 mM MOPS, 1 M KCl, pH 7.0. (b) The  $\alpha$ HL droplet was connected to the first droplet (see inset photo; scale bar is 1 mm), and a DIB was allowed to form. Pore insertion was manifested as stepwise increases in ionic current at  $-50$  mV. (c) The  $\alpha$ HL droplet was then disconnected from the first droplet and moved to the second droplet. The binding of  $\gamma$ CD to the pores is visible as transient current blocks; these events are superimposed on the overall stepwise increases in current caused by pore insertion. (d) After recording from the second droplet, the  $\alpha$ HL droplet was connected to the third droplet. TRIMEB binding caused a larger current block than the  $\gamma$ CD. (e) Finally, the  $\alpha$ HL droplet was reconnected to the first droplet. No binding events can be seen as the pores insert, demonstrating that the  $\alpha$ HL droplet had not been contaminated by the analytes in the second or third droplets.

$\text{Ca}^+$ , and  $\text{Cl}^-$  channels, have been previously studied using planar bilayers, the cumbersome nature of the planar bilayer method hinders progress in this field.<sup>33–40</sup> The ruggedness and long-term stability of the DIB system are ideally suited to address this technology gap. As a demonstration, we screened a droplet containing WT  $\alpha$ HL against an array of three analyte-containing droplets. One droplet contained only buffer (10 mM MOPS, 1 M KCl, pH 7.0), the second contained 50  $\mu$ M  $\gamma$ CD, and the third contained 50  $\mu$ M TRIMEB (permethylated  $\beta$ -cyclodextrin) in the same buffer. The  $\alpha$ HL droplet was placed on the movable electrode. The opposing electrode was common to the three analyte droplets, each of which was placed on a separate “tee” (Figure 5a, Figure 5b–e insets). The  $\alpha$ HL droplet was connected to the first droplet, and an electrical recording

was taken (Figure 5b). Pore insertion was manifested as stepwise increases in ionic current. After recording, the  $\alpha$ HL droplet was disconnected from the first droplet and then connected to the second droplet. Once again, stepwise increases in current indicate the insertion of  $\alpha$ HL pores. In addition, transient partial blockades ( $\sim 60\%$ ) in current are also observed, due to the binding and release of  $\gamma$ CD (Figure 5c). After recording, the  $\alpha$ HL droplet was disconnected from the second droplet and connected to the third droplet (Figure 5d). The TRIMEB binding can be clearly distinguished from the  $\gamma$ CD binding observed previously, since the TRIMEB blocks the current nearly completely. Finally, the  $\alpha$ HL droplet was reconnected to the first droplet and a recording was taken (Figure 5e); the behavior of  $\alpha$ HL was identical to that seen in the initial recording. This demonstrated that the protein-containing droplet had not been contaminated by either of the blocking analytes. The study of ion channel-related disease might be pursued more efficiently through the DIB system. Further, DIBs may prove especially helpful when screening new pharmaceutical candidates for potentially lethal binding or blocking interactions with ion channels.

Here, we have shown that a bilayer spontaneously forms after the connection of two droplets in an oil/lipid bath. Both major classes of membrane protein,  $\alpha$ -helix bundles (BR) and  $\beta$  barrels ( $\alpha$ HL), are able to insert and function in this system. In contrast to the typical planar bilayer lifetime of a few hours,<sup>41</sup> the DIB pairs and networks reproducibly last several days. This ruggedness will enable the study of processes which occur over time periods well beyond the lifetime of a standard planar bilayer. The volume of the droplets used in our experiments was typically 200 nL, which proved to be convenient for handling. However, reducing the volume to the picoliter range should also be possible. Previously, biomimetic fluidic conduits have been formed between vesicle-based protocells to create open, nonselective pathways.<sup>42–44</sup> By contrast, our system would allow picodroplet networks to be built with highly selective or otherwise functional gateways at every interface. Here, we have demonstrated ion-selective and light-sensitive DIB systems, but other properties, such as gating, rectification, and molecular recognition could also be incorporated.

We envision the arrangement of more complex, multifunctional networks as a first step toward the development of an artificial tissue platform. Of immediate interest are electrically propagating systems, such as the heart. DIB networks containing engineered pores that mimic the channels and gap junctions found in cardiac tissue might be arranged in a three-dimensional array to simulate and study the mechanism of electrical impulse propagation.<sup>45</sup> These systems could be divided into regions dedicated to specific functions that are autonomously powered by using one or several “biobatteries.” Since the droplets can be disconnected and interchanged, libraries of mutant proteins could be screened for their effects at specific locations throughout a network.

- (33) Zhang, Y. L.; Dunlop, J.; Dalziel, J. E. *Biosens. Bioelectron.* **2007**, *22*, 1006–1012.  
 (34) Darman, R. B.; Ivy, A. A.; Ketty, V.; Blaustein, R. O. *J. Gen. Physiol.* **2006**, *128*, 687–699.  
 (35) Cannon, B.; Hermansson, M.; Gyorke, S.; Somerharju, P.; Virtanen, J. A.; Cheng, K. H. *Biophys. J.* **2003**, *85*, 933–942.  
 (36) Tulk, B. M.; Kapadia, S.; Edwards, J. C. *Am. J. Physiol.* **2002**, *282*, C1103–C1112.  
 (37) Wartenberg, H. C.; Wartenberg, J. P.; Urban, B. W. *Basic Res. Cardiol.* **2001**, *96*, 645–651.  
 (38) LeMasurier, M.; Heginbotham, L.; Miller, C. J. *Gen. Physiol.* **2001**, *118*, 303–313.  
 (39) Heginbotham, L.; LeMasurier, M.; Kolmakova-Partensky, L.; Miller, C. J. *Gen. Physiol.* **1999**, *114*, 551–559.  
 (40) Picher, M.; Decrouy, A.; Proteau, S.; Rousseau, E. *Biochim. Biophys. Acta: Biomembr.* **1997**, *1328*, 243–260.

- (41) Miller, C. *Ion Channel Reconstitution*; Plenum Press: New York, 1986.  
 (42) Evans, E.; Bowman, H.; Leung, A.; Needham, D.; Tirrell, D. *Science* **1996**, *273*, 933–935.  
 (43) Karlsson, A.; Karlsson, R.; Karlsson, M.; Cans, A. S.; Stromberg, A.; Ryttsen, F.; Orwar, O. *Nature* **2001**, *409*, 150–152.  
 (44) Karlsson, M.; Davidson, M.; Karlsson, R.; Karlsson, A.; Bergenholtz, J.; Konkoli, Z.; Jesorka, A.; Lobovkina, T.; Hurtig, J.; Voinova, M.; Orwar, O. *Annu. Rev. Phys. Chem.* **2004**, *55*, 613–649.  
 (45) Kleber, A. G.; Rudy, Y. *Physiol. Rev.* **2004**, *84*, 431–488.

**Acknowledgment.** We thank R. Madathil, M. Wallace, A. Heron, J. Thompson, and S. White for helpful discussions. The N123R  $\alpha$ HL was made by E. Mikhailova. H.B. is the holder of a Royal Society-Wolfson Research Merit Award. This work was supported by a grant from the Medical Research Council (H.B.), and NIH Grants GM40162 (D.N.) and EY01650 (H.B.).

**Supporting Information Available:** Experimental details including network construction and manipulation, design of recording platforms, and videos. This material is available free of charge via the Internet at <http://pubs.acs.org>.

JA072292A